CAMSAP3 orients the apical-to-basal polarity of microtubule arrays in epithelial cells

Mika Toya[a], Saeko Kobayashi[a], Miwa Kawasaki[a], Go Shioi[b], Mari Kaneko[c], Takashi Ishiuchi[a,1], Kazuyo Misaki[d], Wenxiang Meng[a,2], and Masatoshi Takeichi[a,3]

[a]Laboratory for Cell Adhesion and Tissue Patterning, RIKEN Center for Developmental Biology, Kobe 650-0047, Japan; [b]Genetic Engineering Team, RIKEN Center for Life Science Technologies, Kobe 650-0047, Japan; [c]Animal Resource Development Unit, RIKEN Center for Life Science Technologies, Kobe 650-0047, Japan; and [d]Ultrastructural Research Team, RIKEN Center for Life Science Technologies, Kobe 650-0047, Japan

Contributed by Masatoshi Takeichi, December 2, 2015 (sent for review October 19, 2015; reviewed by Gohta Goshima, Sachiko Tsukita, and Alpha Yap)

Polarized epithelial cells exhibit a characteristic array of microtubules that are oriented along the apicobasal axis of the cells. The minus-ends of these microtubules face apically, and the plus-ends face toward the basal side. The mechanisms underlying this epithelial-specific microtubule assembly remain unresolved, however. Here, using mouse intestinal cells and human Caco-2 cells, we show that the microtubule minus-end binding protein CAMSAP3 (calmodulin-regulated–spectrin-associated protein 3) plays a pivotal role in orienting the apical-to-basal polarity of microtubules in epithelial cells. In these cells, CAMSAP3 accumulated at the apical cortices, and tethered the longitudinal microtubules to these sites. *Camsap3* mutation or depletion resulted in a random orientation of these microtubules; concomitantly, the stereotypic positioning of the nucleus and Golgi apparatus was perturbed. In contrast, the integrity of the plasma membrane was hardly affected, although its structural stability was decreased. Further analysis revealed that the CC1 domain of CAMSAP3 is crucial for its apical localization, and that forced mislocalization of CAMSAP3 disturbs the epithelial architecture. These findings demonstrate that apically localized CAMSAP3 determines the proper orientation of microtubules, and in turn that of organelles, in mature mammalian epithelial cells.

microtubule assembly | microtubule minus-end | intestinal epithelial cell | CAMSAP | Nezha

Microtubules play pivotal roles in fundamental cellular functions, including cell division, intracellular transport, and cell morphogenesis. They are dynamic structures with an intrinsic polarity of rapidly growing plus-ends and slowly growing minus-ends (1). In living cells, the microtubule minus-ends are stabilized by binding to specific molecules or structures, such as the γ-tubulin ring complex located at the centrosome (2). In epithelial cells, however, most microtubules do not emanate from the centrosome; instead, they are aligned along the apicobasal axis with their minus ends facing toward the apical domain (3–5). These observations suggest the presence of unidentified mechanisms that stabilize the minus ends of microtubules at apical regions. Such mechanisms have not yet been identified, although the potential involvement of microtubule-binding proteins, such as ninein, has been suggested (6).

Although many proteins that modulate plus-end dynamics have been identified (7), how the minus-ends are controlled at noncentrosomal sites remains less well understood (2, 8–10). CAMSAP3 (also known as Nezha) is a member of the calmodulin-regulated–spectrin-associated proteins (CAMSAP)/Nezha/Patronin family proteins, which bind and stabilize the minus-ends of microtubules (11–18). In cultured mammalian cells, CAMSAP proteins have been shown to stabilize noncentrosomal microtubules in the cytoplasm or cell junctions (11, 14, 19, 20), suggesting their possible involvement in the spatial regulation of microtubule assembly in polarized cells, such as epithelial-specific longitudinal microtubule alignment.

To date, no study has analyzed CAMSAP function in fully polarized epithelial cells, however. In the present study, we examined whether CAMSAP3 contributes to the epithelial-specific microtubule organization using intestinal epithelial cells. Our results demonstrate that CAMSAP3 plays a key role in tethering microtubules to the apical cortex in epithelial cells, and in turn regulates the positioning of organelles at their cytoplasm.

Results

Loss of Polarized Microtubule Arrays in CAMSAP3-Mutated Epithelial Cells. We mutated mouse *Camsap3* by gene targeting, as depicted in Fig. S1*A*. The resultant mutant mice expressed a C terminus-truncated CAMSAP3 (Fig. S1 *B*–*E*), which lacks the CKK domain essential for the binding of this molecule to the microtubule (11, 12, 14, 15). RT-PCR analysis confirmed that mRNA transcribed from the mutated gene does not cover the exons that encode the CKK domain (Fig. S1 *D* and *E*). We designated the mutated gene as $Camsap3^{tm1Ltm}$, according to the Mouse Genome Informatics guidelines for gene nomenclature; for convenience, we call the mutant allele $Camsap3^{dc}$.

Homozygous $Camsap3^{dc/dc}$ mice were viable, but showed growth defects, whereas heterozygous $Camsap3^{+/dc}$ mice had no such defects (Fig. S1 *F* and *H*). Approximately 15% of the homozygous mutant mice died before postnatal day (P) 30, but the lifespan of the remaining survivors was indistinguishable from that of wild type (WT) and heterozygous mice (Fig. S1*G*). To analyze the phenotypes in polarized epithelia of these mice, we

Significance

Polarization is essential for epithelial cells to exert a variety of functions. Epithelial polarization includes characteristic microtubule array formation. The microtubules are oriented along the apicobasal axis with their minus ends facing apically. The molecules that regulate such epithelial-specific microtubule assembly remain unknown, however. Our study demonstrates that in intestinal epithelial cells, the microtubule minus-end binding protein CAMSAP3 (calmodulin-regulated–spectrin-associated protein 3) tethers noncentrosomal microtubules to the apical cortex, leading to their longitudinal orientation. This mechanism is essential for maintaining epithelial intracellular organization, such as positioning of organelles. Our findings facilitate our understanding of how epithelial cells acquire polarized structures, which are crucial for their physiological functions.

Author contributions: M. Toya and M. Takeichi designed research; M. Toya, S.K., M. Kawasaki, and K.M. performed research; T.I. contributed new reagents/analytic tools; G.S. and M. Kaneko generated knockout mice; K.M. performed electron microscopy; W.M. generated KO mice and conducted preliminary experiments; M. Toya and M. Takeichi analyzed data; and M. Toya and M. Takeichi wrote the paper.

Reviewers: G.G., Nagoya University; S.T., Osaka University; and A.Y., Institute for Molecular Bioscience, University of Queensland.

The authors declare no conflict of interest.

[1]Present address: Division of Epigenomics and Development, Medical Institute of Bioregulation, Kyushu University, Fukuoka 812-8582, Japan.

[2]Present address: State Key Laboratory of Molecular Developmental Biology, Institute of Genetics and Developmental Biology, Chinese Academy of Sciences, Beijing 100101, China.

[3]To whom correspondence should be addressed. Email: takeichi@cdb.riken.jp.

This article contains supporting information online at www.pnas.org/lookup/suppl/doi:10.1073/pnas.1520638113/-/DCSupplemental.

www.pnas.org/cgi/doi/10.1073/pnas.1520638113

used the small intestinal epithelium at around P21, focusing on absorptive cells located at the lateral walls of villi (Fig. 1*A*, *Top*). In immunofluorescence staining for CAMSAP3 in WT intestines, CAMSAP3 was detected as punctate signals, and these punctae were concentrated at apical cortical areas of the cells, with additional scattering at deeper regions of the cytoplasm (Fig. 1*A*, *Left*). In contrast with previous observations (11), however, we did not detect CAMSAP3 from cell–cell junctions in these intestinal cells (see below). Double staining for CAMSAP3 and F-actin revealed CAMSAP3 punctae overlapping the basal edges of the apical actin meshwork (Fig. 1*A*, *Left*), which organizes microvilli and terminal web (21, 22). The apical concentration of CAMSAP3 disappeared in homozygous mutant cells (Fig. 1*A*, *Right*), although apical F-actin was distributed normally in these cells, indicating that the mutated CAMSAP3 failed to concentrate at these sites.

We then analyzed microtubule distribution by stimulated emission-depletion (STED) super-resolution microscopy, using sections double-immunostained for α-tubulin and CAMSAP3. In WT intestinal absorptive cells, microtubules were aligned along the apicobasal axis, as seen in other epithelial cells. The apical ends of these microtubules terminated at distinct CAMSAP3 punctae (Fig. 1*B*, *Left*). In the absorptive cells of homozygous mutant mice, the apicobasal orientation of microtubules was no longer observed; many of the microtubules exhibited a wavy appearance, with a loss of specific directionality (Fig. 1*B*, *Right*). Top-down views of *Camsap3*$^{dc/dc}$ cells confirmed that the microtubules did not terminate perpendicularly at the apical cortex, but instead tended to be arranged horizontally along the apical membrane (Fig. 1*C*). We also noticed a decreased overall microtubule density in *Camsap3*$^{dc/dc}$ cells (Fig. 1*D*). In contrast, heterozygous mutant cells exhibited normal microtubule organization (Fig. S1*I*), suggesting that the truncated CAMSAP3 molecules have no dominant-negative effects. (See Fig. S4 for further characterization of the CKK domain-deleted CAMSAP3.) Given the previous observation that CAMSAP3 selectively binds to the minus ends of microtubules (11–16), our results suggest that CAMSAP3, concentrated at apical cortices, tethers microtubules to these sites through the binding to their minus-ends, ensuring the longitudinal alignment of this cytoskeleton, and that this function of CAMSAP3 is abolished in the absence of the CKK domain.

Misplacement of Organelles in CAMSAP3-Mutated Cells. We next investigated for any cellular architecture impairment from the *Camsap3* mutation. We found disordered nuclear positioning, along with reduced cell height, in *Camsap3*$^{dc/dc}$ cells. In WT or heterozygous mutant cells, the nucleus was located in an invariable position, biased toward the basal side of the cytoplasm (Fig. 2*A*, *Left* and Fig. S1*I*). In contrast, the positions of nuclei varied in homozygous mutant cells; in many cells, the nucleus was detected close to the apical cortex (Fig. 2*A*, *Right*). Golgi complexes also were atypically located in *Camsap3*$^{dc/dc}$ cells; instead of the normal WT position just above the nucleus, they were often detected elsewhere, even sometimes below the nucleus (Fig. 2*B*). These findings suggest that intracellular polarity, which is recognized by organelle positioning, was disturbed when normal CAMSAP3 function was lost. Electron microscopy images also showed that mitochondrial elongation along the longitudinal axis, which occurs in WT cells, tended to be suppressed in *Camsap3*$^{dc/dc}$ cells (Fig. S2*A*).

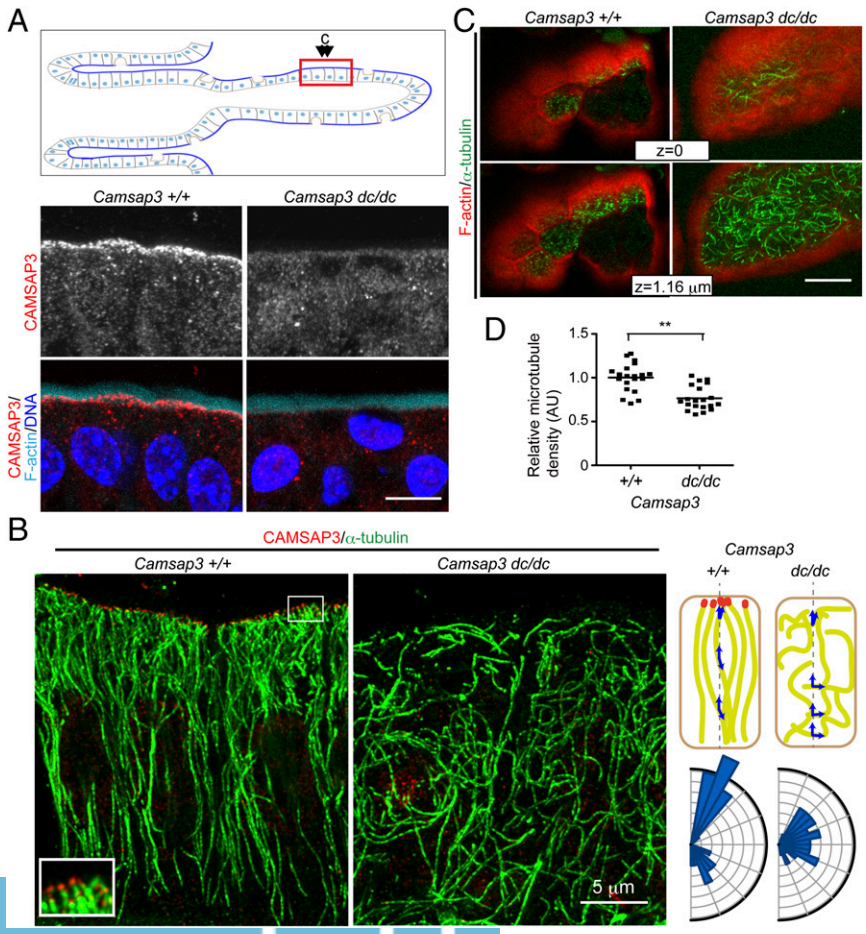

Fig. 1. Localization of CAMSAP3 and microtubules in small intestinal epithelial cells of WT (+/+) and *Camsap3* mutant (*dc/dc*) mice. (*A*) Vertical view of intestinal epithelial layers. The areas analyzed are indicated with a square on a schematic drawing of a villus. The direction of views in *C* is indicated as well. (*Lower*) Cells stained for the molecules indicated. (*B*) Images obtained by STED super-resolution microscopy. Deconvolved images are projected. (*Inset*) Enlargement of the boxed region. (*Right*) Quantification of microtubule orientation. Using multiple optical sections of the images, vertical lines were arbitrarily drawn along the apicobasal axis of the cells, and the angles of microtubules that cross the lines were measured at the right side of the line over 40 crossing points. (*C*) Top views of cells optically sectioned at two different focal planes in the apical region marked by F-actin staining. (Scale bars: 10 μm.) (*D*) Relative microtubule density. Immunofluorescence signals detecting microtubules were binarized using images optically projected in a 1.45-μm thickness, and signal intensity was measured at the whole area of each cell. The relative ratios of microtubule signals to the whole cell area are plotted. Lines indicate mean values. A total of 20 cells from two animals were measured. $^{**}P < 0.0001$, Student's *t* test.

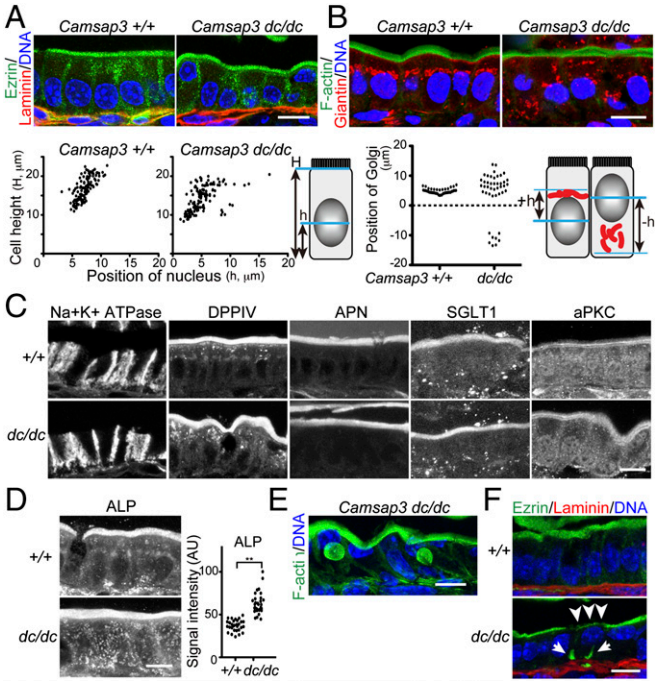

Fig. 2. Architecture of small intestinal epithelial cells in WT (+/+) and *Camsap3* mutant (*dc/dc*) mice. (*A*) Apical structures and the basement membrane were immunostained for ezrin and laminin, respectively, and nuclei were visualized by DAPI staining. Cell height (H) and nuclear positions (h) were measured as explained in the drawing (n >120 cells, two animals for each sample). (*B*) Golgi, apical structures, and nuclei were visualized by staining for Giantin, F-actin, and DAPI, respectively. Golgi complexes are located either above or below the nucleus. The distances between the middle portion of nucleus and the most apically (+h) or basally (–h) located Giantin-positive fragments of Golgi were measured using 44 cells for each specimen, as explained in the drawing. (*C*) Localization of Na^+K^+ ATPase, DPPIV, APN, SGLT1, and aPKC. (*D*) Localization of ALP. The graph shows the variation in cytoplasmic ALP. Immunosignals for ALP were measured in the entire cytoplasm of each cell, and the relative intensities of the signals obtained from multiple cells are plotted (n = 30 cells). $^{**}P < 0.0001$, Student's t test. (*E*) F-actin inclusion bodies in *Camsap3*$^{dc/dc}$ cells. (*F*) Mislocalization of ezrin in mutant cells (arrows). Apical ezrin immunoreactivity is reduced in the same cell (arrowheads). (Scale bars: 10 μm.)

Despite the observed disturbance in organelle positioning, apicobasolateral membrane polarity appeared to be normal in *Camsap3*$^{dc/dc}$ cells. A basolateral membrane protein, sodium-potassium ATPase, was detected in a similar pattern in WT and mutant cells. The positioning of three apical membrane proteins—dipeptidyl peptidase IV (DPPIV/Dpp4), aminopeptidase N (APN), and sodium-dependent glucose transporter (SGLT1)—was also normal in *Camsap3*$^{dc/dc}$ cells (Fig. 2*C*). Distribution of aPKC (an apical cortex protein), which marks the apical cortex, also did not change in the mutant cells (Fig. 2*C*). Electron microscopy confirmed that the brush borders characterizing the apical surface of intestinal absorptive cells formed normally in *Camsap3*$^{dc/dc}$ mice (Fig. S2*A*). We did notice, however, that another apical membrane marker, alkaline phosphatase (ALP), tended to internalize in *Camsap3*$^{dc/dc}$ cells, although its dominant localization at the apical membranes was unchanged (Fig. 2*D*). Furthermore, in a restricted population of homozygous mutant cells, we detected large F-actin–positive vesicles within the cytoplasm (Fig. 2*E*). We also noticed that ezrin, an ERM family protein that normally localizes only at the brush border and terminal web (23), was mislocalized to basal regions in a certain fraction of the mutant cells (Fig. 2*F*). This mislocalization of ezrin was accompanied by a reduction in apical ezrin immunosignals. These observations suggest that the apical membranes in *Camsap3*$^{dc/dc}$ are less stable than those in WT cells, despite their normal appearance.

We also examined whether CAMSAP3 mutation affected cell junction formation. Immunostaining for ZO-1 (a tight junction protein) and E-cadherin (an adherens junction protein) showed that these proteins normally distribute along cell–cell contacts in *Camsap3*$^{dc/dc}$ cells (Fig. S3*A*). Electron microscopy also indicated that these junctions were not structurally affected by CAMSAP3 mutation (Fig. S2*B*). These results are consistent with the observation that CAMSAP3 is absent in the junctions of mouse intestinal absorptive cells (Fig. S3*A*).

Disorganization of Epithelial Architecture in CAMSAP3-Depleted Caco-2 Cells. For further analysis of CAMSAP3 function, we used human intestinal Caco-2 cells. We cultured these cells on polycarbonate membranes, which allowed their growth into cuboidal or columnar epithelial cell layers. As reported previously (11), in these cells, CAMSAP3 was detected from the apical adherens junctions (zonula adherens), as well as from nonjunctional cortical areas. On maturation of the cell sheets, however, junctional CAMSAP3 gradually decreased, and nonjunctional CAMSAP3 increased. By day 20 in culture, CAMSAP3 became undetectable at the cell junctions, localizing only on apical cortices, as observed in the intestinal absorptive cells (Fig. S3*B*). PLEKHA7, identified as a partner for CAMSAP3 at cell junctions (11), was expressed not only in early cultures, but also in mature sheets (Fig. S3*C*), suggesting that the junctional localization of CAMSAP3, including its binding to PLAKHA7, is regulated in a cell density-dependent manner.

We then generated stable CAMSAP3 knockdown clones of Caco-2 cells using specific shRNAs. These "shRNAi CAMSAP3" cells, in which CAMSAP3 was depleted (Fig. S3*D*), organized into flatter sheets compared with control cells, with a concomitant widening of the apical areas as well as a distortion of cell–cell contact morphology, as assessed by ZO-1 immunostaining (Fig. S3*B*). By 20 d, however, CAMSAP3-depleted cells grew into layers of a height comparable to that of control cells, although nuclear positioning appeared abnormal in these layers; the distorted cell–cell contacts were also restored to nearly normal. These results suggest that CAMSAP3 is involved in junction formation at low cell densities, but this function becomes less important at high densities. The mouse intestinal absorptive cells likely are equivalent to mature Caco-2 cell layers, given that their junctions were not affected by CAMSAP3 mutation.

To evaluate microtubules and organelles in Caco-2 cells, we cultured them in Matrigel (BD Biosciences), in which cells form spherical cysts with a central lumen and apicobasal polarity, which allowed us to examine the polarized subcellular structures from lateral sides. In control cysts, CAMSAP3 was concentrated at both apical cell junctions and nonjunctional apical cortices (Fig. 3*A*, *Left*), indicating that the cell layers forming cysts correspond to premature epithelial sheets observed in polycarbonate membrane cultures. Live imaging of CAMSAP3-GFP expressed in the cysts confirmed that CAMSAP3 accumulated stably at the apical cortex, although a fraction of CAMSAP3 punctae located in deeper regions appeared mobile (Movie S1). In these cysts, microtubules were aligned along the apicobasal axis, and the Golgi was positioned above the nucleus (Fig. 3*B*, *Left*); however, in shRNAi CAMSAP3 cells, the longitudinal distribution of microtubules was distorted, and the stereotypic positions of nuclei and Golgi were disturbed (Fig. 3*B*, *Right*). Immunostaining for E-cadherin, which delineates the apical-to-lateral cell–cell contacts, indicated distorted cell–cell arrangement in CAMSAP3-depleted cysts as well (Fig. 3*C*).

To analyze the apical architecture in these cells, we immunostained cysts for ZO-1 and aPKC and found that, although the majority of normal Caco-2 cysts have a single lumen, which is either open or closed, cysts with multiple lumens increased when CAMSAP3 was depleted (Fig. 3*D*). This abnormality was rescued

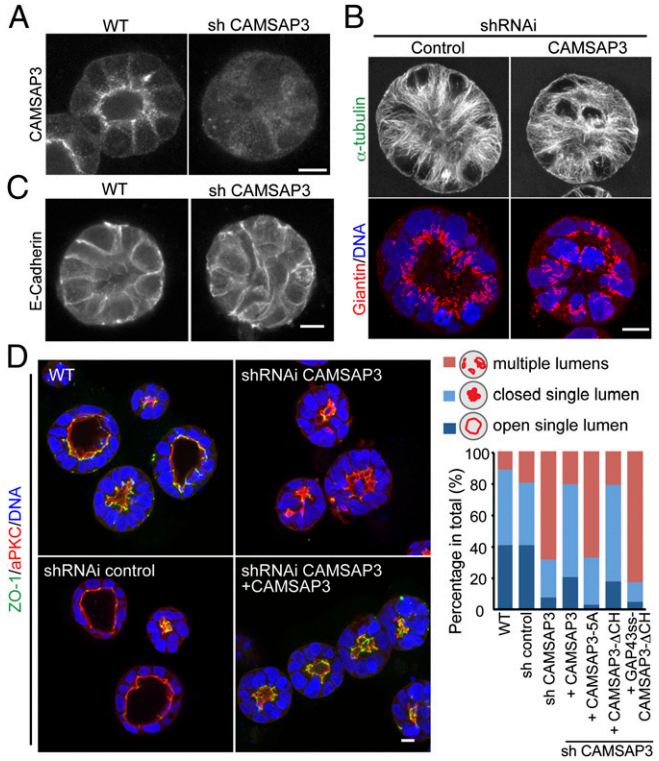

Fig. 3. Effects of CAMSAP3 depletion on the subcellular architecture of Caco-2 cysts. (*A*–*C*) Localization of CAMSAP3 (*A*); microtubules, Golgi, and nuclei (*B*); and E-cadherin (*C*) in WT, control shRNA-expressing (shRNAi control), and CAMSAP3 shRNA-expressing (shRNAi CAMSAP3) Caco-2 cysts. (*D*) Localization of ZO-1, aPKC, and nuclei in Caco-2 cysts of WT cells, shRNAi control cells, shRNAi CAMSAP3 cells, and shRNAi CAMSAP3 cells into which *Camsap3* cDNA is integrated (shRNAi CAMSAP3 + CAMSAP3). Lumen formation was categorized as shown in the drawing, in which "multiple" was defined as more than one and "open" and "closed" lumens were defined as those with and without an open space, respectively. Multiple lumens cover both the open and closed lumens. The ratio of each lumen type in the cysts expressing only shRNA (control or CAMSAP3 shRNA) or coexpressing CAMSAP3 shRNA and additional constructs indicated is shown in the graph. The fifth to seventh lanes from the left show the effects of CAMSAP3-5A (Fig. 5*D*), and CAMSAP3-ΔCH and GAP43ss-CAMSAP3-ΔCH (Fig. 5*H*) expression in shRNAi CAMSAP3 cells. More than 120 cysts were counted for each specimen.

by reexpression of CAMSAP3. Thus, in CAMSAP3-depleted Caco-2 cells, defects in cell–cell contacts and apical domain architecture were observed in addition to the mispositioning of organelles.

We also used Caco-2 cysts to check whether the C terminus-truncated CAMSAP3 mutant, expressed in the *Camsap3*$^{dc/dc}$ intestine, retained any active role in epithelial architecture. We generated a CKK domain-truncated CAMSAP3 (ΔCKK), which is nearly equivalent to the mutant molecule expressed in the *Camsap3*$^{dc/dc}$ mice (Fig. S4 *A* and *B*). When ΔCKK was expressed in Caco-2 cells, it distributed diffusely in the cytoplasm (Fig. S4 *C*, *D*, and *H*), and its expression in shRNAi CAMSAP3 cells did not rescue the abnormal organization of microtubules and organelles that occurs in these cells (Fig. S4*F*). We also found that overexpression of ΔCKK in WT cells did not affect the longitudinal assembly of microtubules (Fig. S4*G*) or the localization of Golgi, endogenous CAMSAP3, or ZO-1 (Fig. S4*H*). These results confirm that CKK domain-deleted CAMSAP3s are functionally inert as far as the phenomena investigated here are concerned.

Microtubule Plus-End Growth from Atypical Sites in CAMSAP3-Depleted Cells. To evaluate how microtubule plus-ends grow in CAMSAP-depleted cells, we stably expressed EB3-GFP, a microtubule plus-end tracking protein (24), in control and shRNAi CAMSAP3 Caco-2 cells and collected its trajectories through live imaging, using their cysts. In control cells, most of the EB3-GFP signals ran in an apical-to-basal direction (Fig. 4*A*, *Left* and Movie S2). In contrast, the angle of EB3-GFP trajectories varied in shRNAi CAMSAP3 cells (Fig. 4*A*, *Right* and Movie S3). We also found that some EB3-GFP signals arose from the basal areas of cells, in addition to their radiation from apical sites, in shRNAi CAMSAP3 cells (Movie S4). Immunostaining for γ-tubulin, a component of the microtubule nucleator that accumulates at the centrosome, showed that although the centrosomes always localized at apical regions in WT cells, they were often mislocated to basolateral regions in CAMSAP3-depleted cells (Fig. 4*B*). These results suggest that in CAMSAP3-deficient cells, microtubules grow from erroneous positions, which perhaps include mislocated centrosomes.

Involvement of the CC1 Domain in the Apical Localization of CAMSAP3. We next explored the mechanisms by which CAMSAP3 concentrates at the apical cortex. Because CAMSAP3 punctae overlap with F-actin networks at the apical cortex (Fig. 1*A*), we first examined the effects of actin depolymerization induced by latrunculin A treatments on CAMSAP3 distribution using the polycarbonate membrane cultures. In latrunculin A-treated cells, both junctional and cortical F-actin filaments diminished, and simultaneously CAMSAP3 punctae disappeared from the cortical regions, although they were still detectable in junctional areas to some extent (Fig. S5*A*). This observation suggests that F-actin or F-actin–bound proteins are involved in the anchoring of CAMSAP3 to the apical cortex.

We next investigated which domains of CAMSAP3 are responsible for its apical localization. The CC1 domain of CAMSAP1 has been reported to interact with βII-spectrin (25). The amino acid sequence crucial for this interaction within the CC1 domain was identified as LEEK (25), and this sequence with additional R (i.e., LEEKR) is conserved in CAMSAP3 (Fig. 5*A*). We generated a CAMSAP3 mutant, designated CAMSAP3-5A, in which this sequence was replaced with AAAAA, and integrated its GFP-tagged form (CAMSAP3-5A-GFP) into shRNAi CAMSAP3 Caco-2 cells. These cells were cultured in Matrigel. In the cysts thus formed, CAMSAP3-5A-GFP was detected in a punctum form, and these punctae associated with microtubule ends (Fig. 5 *B* and *C*), suggesting that this mutant CAMSAP3 retains the ability to interact with microtubules. However, the mutant never localized to specific regions, but remained distributed throughout the cytoplasm, suggesting that the CC1 domain is required for the apical localization of CAMSAP3. We also examined localization of the apical markers ZO-1 and aPKC in shRNAi CAMSAP3 Caco-2 cells into which CAMSAP3-5A or control CAMSAP3 was introduced, and found

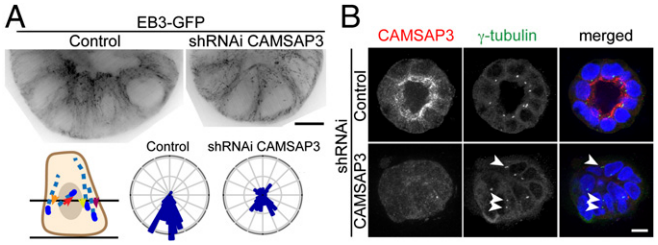

Fig. 4. Effects of CAMSAP3 depletion on microtubule plus-end behavior in Caco-2 cysts. (*A*) Inverted live images of EB3-GFP trajectories collected by 5-min recordings as 43 frames. The orientation of EB3-GFP trajectories was quantified by measuring their angles to the line drawn parallel to the basal surface of the cell. The measurement was made at around the middle level of the cells. Cells were grown for 7 d in Matrigel. (*B*) Centrosomes visualized by immunostaining for γ-tubulin in control and CAMSAP3-depleted cells. Arrows point to examples of aberrantly located centrosomes. (Scale bars: 10 μm.)

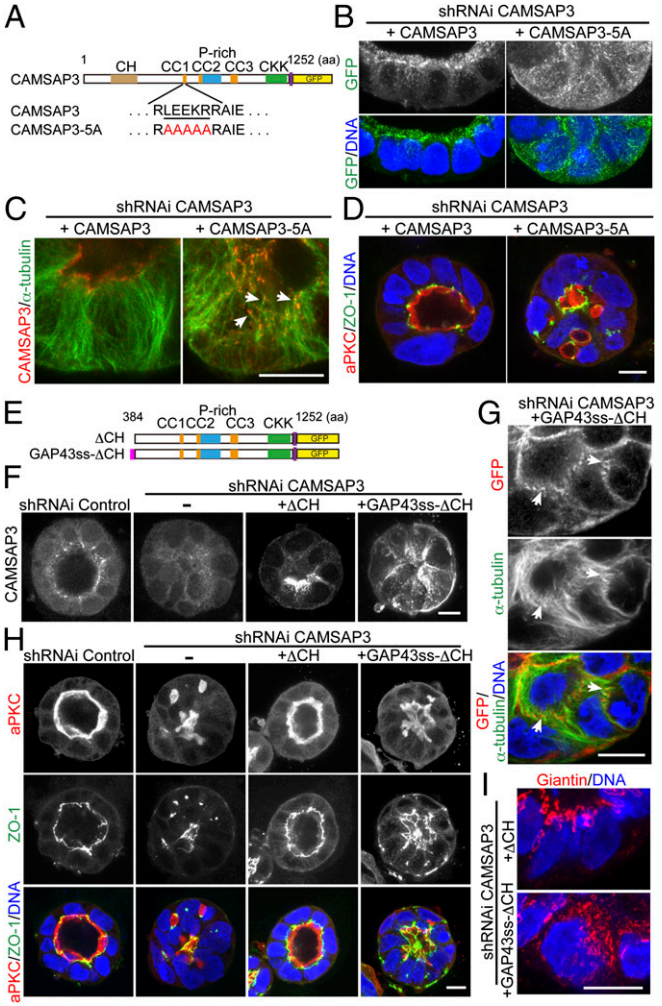

Fig. 5. Effects of forced mislocalization of CAMSAP3 on the architecture of Caco-2 cysts. (*A*) Amino acid sequences in the CC1 domain of CAMSAP3. Amino acid residues conserved among CAMSAP proteins are underscored. Mutated amino acids are shown in red. CH, calponin homology domain; CC, coiled-coil domain; P-rich, proline-rich stretch; CKK, C-terminal domain common in CAMSAPs; purple line, long linker sequence. (*B* and *C*) Localization of CAMSAP3 or CAMSAP3-5A in shRNAi CAMSAP3 cysts, into which cDNA encoding CAMSAP3-GFP or CAMSAP3-5A-GFP is integrated. Cysts were immunostained for the proteins indicated. Arrows point to examples of CAMSAP3 punctae associated with an end of microtubules. (*D*) Localization of ZO-1, aPKC, and nuclei in cysts of shRNAi CAMSAP3 cells, into which CAMSAP3 or CAMSAP3-5A cDNA is integrated. Quantification of multiple lumen formation in these specimens is shown in Fig. 3*D*. (Scale bars: 10 μm.) (*E*) Structures of CAMSAP3-ΔCH (ΔCH) and its membrane-bound form GAP43ss-ΔCH. The magenta line indicates the lipid-interacting signal sequence of GAP43. (*F*) Immunostaining for CAMSAP3 in a cyst of shRNAi control cells, shRNAi CAMSAP3 cells (–), or shRNAi CAMSAP3 cells into which ΔCH or GAP43ss-ΔCH is integrated. Variations in the intensity of immunosignals for CAMSAP3 among the cells expressing ΔCH or GAP43ss-ΔCH is due to heterogeneity in the expression level of exogenous proteins in these transfectants. (*G*) Double-immunostaining for GFP (GAP43ss-ΔCH) and α-tubulin in shRNAi CAMSAP3 cysts into which GAP43ss-ΔCH is integrated. Arrows indicate examples of CAMSAP3 punctae associated with microtubules. (*H*) Localization of aPKC and ZO-1 in the cysts expressing the indicated constructs. Quantification of multiple lumen formation in these specimens is shown in Fig. 3*D*. (*I*) Localization of Giantin-positive Golgi complexes in shRNAi CAMSAP3 cysts expressing ΔCH or GAP43ss-ΔCH.

that CAMSAP3-5A expression could not rescue the CAMSAP3 depletion phenotypes (Fig. 5*D*, and Fig. 3*D* for quantification). These observations suggest that CAMSAP3 needs to localize at the apical cortex to maintain normal epithelial architecture.

Given that the C terminus-truncated CAMSAP3 mutant encoded by *Camsap3*^{dc} as well as ΔCKK do not accumulate at the apical cortex, this domain also appears to be involved in apical localization. Because the CKK is a microtubule-binding domain, we examined the effect of nocodazole, an inhibitor of microtubule polymerization, on CAMSAP3 localization and found that nocodazole treatments abolished not only the apical localization of CAMSAP3, but also its punctate appearance (Fig. S5*B*). These findings suggest that CAMSAP3 requires interaction with microtubules via the CKK domain for apical accumulation.

Mislocalization of CAMSAP3 Perturbs Epithelial Architecture. To further verify the importance of the apical localization of CAMSAP3, we manipulated the localization of CAMSAP3 proteins by constructing a membrane-anchoring form of CAMSAP3. We chose an N terminus-truncated CAMSAP3 construct (ΔCH), which has intracellular behavior indistinguishable from that of WT CAMSAP3 (Fig. S4 *A*–*E*) and is capable of binding to the minus-ends (11). We fused ΔCH with a membrane-interacting signal sequence of growth-associated protein 43 (GAP43ss) to make GAP43ss-ΔCH (Fig. 5*E*), and stably expressed the GFP-tagged GAP43ss-ΔCH in shRNAi CAMSAP3 cells. As a control, we expressed GFP-tagged ΔCH in these cells. These cells were immunostained to detect CAMSAP3 or GFP. In ΔCH-expressing cells, CAMSAP3 concentrated at apical areas, as expected. In contrast, in GAP43ss-ΔCH–expressing cells, CAMSAP3 signals were localized not only at apical poles, but also at their basolateral membranes (Fig. 5*F*). In these cells, a fraction of microtubules associated with GAP43ss-ΔCH signals at basolateral membranes (Fig. 5*G*).

We then examined ZO-1 and aPKC localization in shRNAi CAMSAP3 cells expressing ΔCH or GAP43ss-ΔCH, and found that although ΔCH expression restored the normal distribution of these molecules to Caco-2 cysts, GAP43ss-ΔCH expression did not (Fig. 5*H*, and Fig. 3*D* for quantification). Golgi were also mispositioned in GAP43ss-ΔCH–expressing cells, but not to a significant degree in ΔCH-expressing cells (Fig. 5*I*). These findings indicate that when CAMSAP3 is forced to mislocalize, it cannot support the formation of normal epithelial structures.

Discussion

How microtubules are assembled with the minus-ends oriented toward the apical membranes in polarized epithelial cells has been a long-standing question. The present study provides evidence that apically localized CAMSAP3 functions to tether microtubules to the apical pole of cells (Fig. S6). Given the previous finding that CAMSAP3 or its *Drosophila* homolog Patronin (11, 13–15, 19) binds the minus ends of microtubules, it is likely that CAMSAP3 holds microtubules via this mechanism at the apical cortex. Arrays of microtubules still formed in the absence of functional CAMSAP3, however. Growth of these microtubules is likely regulated by centrosomes or by other organelles known to nucleate or anchor microtubules (26–28). In support of this idea, we detected radial emanation of EB3 comets from various places in CAMSAP3-depleted cells. CAMSAP2, which was not studied here, also may contribute to the microtubule assembly in these cells, as reported previously (19).

How is CAMSAP3 recruited to the apical cortex? We found that the CC1 domain is responsible for its apical localization. Identifying the targets for CC1 is a topic for future studies, however. The CKK domain is also involved in the apical localization of CAMSAP3. Our results suggest that the interaction of CAMSAP3 with microtubules via the CKK domain is a prerequisite for its localization to apical poles. To confirm the role of apical localization of CAMSAP3, we investigated the effects of forced mislocalization of CAMSAP3 in Caco-2 cysts, finding that mislocalized CAMSAP3 failed to rescue the CAMSAP3 knockdown phenotypes. These results support the idea that CAMSAP3 must localize at the apical regions in epithelial cells to control their normal architecture.

CAMSAP3 dysfunction led to various defects in cell architecture. In *Camsap3*$^{dc/dc}$ intestinal cells, the positioning of nuclei and Golgi and shaping of mitochondria were impaired, suggesting that the CAMSAP3-derived microtubules play a substantial role in proper arrangement of these organelles. These organelles are known to interact with microtubules via various mechanisms (28–30), which may serve to properly arrange the organelles via CAMSAP3-derived microtubules. Notably, the apical membrane architecture was little affected in *Camsap3*$^{dc/dc}$ intestinal cells. This suggests that the longitudinal microtubule arrays established by CAMSAP3 are not essential for maintaining apical plasma membrane integrity, consistent with the view that microtubules are not absolutely required for the transport of membrane proteins from Golgi (31). Nevertheless, the occasional mislocalization of apical structures in *Camsap3*$^{dc/dc}$ cells suggests that the CAMSAP–microtubule system is required for stabilization.

In CAMSAP3-depleted Caco-2 cysts, we found additional defects, including disorganized cell arrangement and multiple lumen formation. Because CAMSAP3 localizes at both the apical junctions and cortices in Caco-2 cysts, the phenotypes observed in the CAMSAP3-depleted cysts were likely a mixture of defects derived from the two structures. On the other hand, intracellular defects, such as Golgi displacement, were commonly observed in both the mouse intestinal and Caco-2 systems, suggesting that these are basic defects brought about by cortical CAMSAP3 loss.

Although CAMSAP3 deficiency-induced microtubule misassembly led to various cytological defects, the majority of CAMSAP3 mutant mice survived, indicating that the observed defects are not lethal to animals. Nevertheless, we found growth retardation in these mice, implying that the CAMSAP3-mediated control of microtubules is important for health maintenance. Because CAMSAP3 is expressed in various organs, our future studies will include analyses of the organs involved in growth retardation and the physiological functions impaired in mutant animals.

Materials and Methods

Mice. We designed a target vector to mutate *Camsap3*/*Nezha* (accession no. CDB0716K; www2.clst.riken.jp/arg/mutant%20mice%20list.html) by replacing the 14th through 17th exons, which correspond to the end of *Camsap3* gene, with the Neo selection cassette. Heterozygous mice were crossed with β-actin Cre transgenic mice (32), to remove the Neo cassette and the 14th to 17th exons through Cre/loxP-mediated excision. Mice were further backcrossed with the C57BL/6N line. The phenotypes observed were essentially identical in F1–F4 generations. The experiments using mice were approved by the Institutional Animal Care and Use Committee of the RIKEN Center for Developmental Biology, and were performed in accordance with protocols provided by this committee.

Cell Culture, Plasmids, and Transfection. Detailed information is provided in *SI Materials and Methods*.

ACKNOWLEDGMENTS. We thank Y. Mimori-Kiyosue for the EB3 construct; A. Harada, S. Hayashi, T. Uesaka, T.S. Kitajima, S. Nakagawa, and S. Kuraku for discussions; M. Sato for a critical reading of the manuscript; and H. Saitou, H. Sylvain, S. Morishita, and H. Yamaguchi for technical support. STED microscopy was supported by Leica Microsystems K.K. Other imaging experiments were performed at the Riken Kobe Imaging Facility. This work was supported by a Grant-in-Aid for Specially Promoted Research (Grant 20002009) and a Grant-in-Aid for Scientific Research (S) (Grant 25221104) (to M. Takeichi), and a Grant-in-Aid for Scientific Research (C) (Grant 25440094) (to M. Toya), all from the Japan Society for Promotion of Science.

1. Desai A, Mitchison TJ (1997) Microtubule polymerization dynamics. *Annu Rev Cell Dev Biol* 13:83–117.
2. Dammermann A, Desai A, Oegema K (2003) The minus-end in sight. *Curr Biol* 13(15): R614–R624.
3. Bacallao R, et al. (1989) The subcellular organization of Madin–Darby canine kidney cells during the formation of a polarized epithelium. *J Cell Biol* 109(6 Pt 1):2817–2832.
4. Mogensen MM, Tucker JB, Stebbings H (1989) Microtubule polarities indicate that nucleation and capture of microtubules occurs at cell surfaces in *Drosophila*. *J Cell Biol* 108(4):1445–1452.
5. Troutt LL, Burnside B (1988) The unusual microtubule polarity in teleost retinal pigment epithelial cells. *J Cell Biol* 107(4):1461–1464.
6. Moss DK, et al. (2007) Ninein is released from the centrosome and moves bi-directionally along microtubules. *J Cell Sci* 120(Pt 17):3064–3074.
7. Akhmanova A, Steinmetz MO (2008) Tracking the ends: A dynamic protein network controls the fate of microtubule tips. *Nat Rev Mol Cell Biol* 9(4):309–322.
8. Jiang K, Akhmanova A (2011) Microtubule tip-interacting proteins: A view from both ends. *Curr Opin Cell Biol* 23(1):94–101.
9. Mimori-Kiyosue Y (2011) Shaping microtubules into diverse patterns: Molecular connections for setting up both ends. *Cytoskeleton (Hoboken)* 68(11):603–618.
10. Akhmanova A, Hoogenraad CC (2015) Microtubule minus end–targeting proteins. *Curr Biol* 25(4):R162–R171.
11. Meng W, Mushika Y, Ichii T, Takeichi M (2008) Anchorage of microtubule minus ends to adherens junctions regulates epithelial cell–cell contacts. *Cell* 135(5):948–959.
12. Baines AJ, et al. (2009) The CKK domain (DUF1781) binds microtubules and defines the CAMSAP/ssp4 family of animal proteins. *Mol Biol Evol* 26(9):2005–2014.
13. Goodwin SS, Vale RD (2010) Patronin regulates the microtubule network by protecting microtubule minus ends. *Cell* 143(2):263–274.
14. Jiang K, et al. (2014) Microtubule minus-end stabilization by polymerization-driven CAMSAP deposition. *Dev Cell* 28(3):295–309.
15. Hendershott MC, Vale RD (2014) Regulation of microtubule minus-end dynamics by CAMSAPs and Patronin. *Proc Natl Acad Sci USA* 111(16):5860–5865.
16. Richardson CE, et al. (2014) PTRN-1, a microtubule minus end-binding CAMSAP homolog, promotes microtubule function in *Caenorhabditis elegans* neurons. *eLife* 3:e01498.
17. Goshima G, et al. (2007) Genes required for mitotic spindle assembly in *Drosophila* S2 cells. *Science* 316(5823):417–421.
18. Wang H, Brust-Mascher I, Civelekoglu-Scholey G, Scholey JM (2013) Patronin mediates a switch from kinesin-13–dependent poleward flux to anaphase B spindle elongation. *J Cell Biol* 203(1):35–46.
19. Tanaka N, Meng W, Nagae S, Takeichi M (2012) Nezha/CAMSAP3 and CAMSAP2 cooperate in epithelial-specific organization of noncentrosomal microtubules. *Proc Natl Acad Sci USA* 109(49):20029–20034.
20. Nagae S, Meng W, Takeichi M (2013) Non-centrosomal microtubules regulate F-actin organization through the suppression of GEF-H1 activity. *Genes Cells* 18(5):387–396.
21. Bretscher A, Weber K (1978) Localization of actin and microfilament-associated proteins in the microvilli and terminal web of the intestinal brush border by immunofluorescence microscopy. *J Cell Biol* 79(3):839–845.
22. Hull BE, Staehelin LA (1979) The terminal web: A reevaluation of its structure and function. *J Cell Biol* 81(1):67–82.
23. Berryman M, Franck Z, Bretscher A (1993) Ezrin is concentrated in the apical microvilli of a wide variety of epithelial cells, whereas moesin is found primarily in endothelial cells. *J Cell Sci* 105(Pt 4):1025–1043.
24. Stepanova T, et al. (2003) Visualization of microtubule growth in cultured neurons via the use of EB3-GFP (end-binding protein 3-green fluorescent protein). *J Neurosci* 23(7):2655–2664.
25. King MD, et al. (2014) A conserved sequence in calmodulin regulated spectrin-associated protein 1 links its interaction with spectrin and calmodulin to neurite outgrowth. *J Neurochem* 128(3):391–402.
26. Lechler T, Fuchs E (2007) Desmoplakin: An unexpected regulator of microtubule organization in the epidermis. *J Cell Biol* 176(2):147–154.
27. Saxton WM, Hollenbeck PJ (2012) The axonal transport of mitochondria. *J Cell Sci* 125(Pt 9):2095–2104.
28. Zhu X, Kaverina I (2013) Golgi as an MTOC: Making microtubules for its own good. *Histochem Cell Biol* 140(3):361–367.
29. Tapley EC, Starr DA (2013) Connecting the nucleus to the cytoskeleton by SUN-KASH bridges across the nuclear envelope. *Curr Opin Cell Biol* 25(1):57–62.
30. Gundersen GG, Worman HJ (2013) Nuclear positioning. *Cell* 152(6):1376–1389.
31. Matter K, Bucher K, Hauri HP (1990) Microtubule perturbation retards both the direct and the indirect apical pathway but does not affect sorting of plasma membrane proteins in intestinal epithelial cells (Caco-2). *EMBO J* 9(10):3163–3170.
32. Meyers EN, Lewandoski M, Martin GR (1998) An Fgf8 mutant allelic series generated by Cre- and Flp-mediated recombination. *Nat Genet* 18(2):136–141.
33. Ishiuchi T, Misaki K, Yonemura S, Takeichi M, Tanoue T (2009) Mammalian Fat and Dachsous cadherins regulate apical membrane organization in the embryonic cerebral cortex. *J Cell Biol* 185(6):959–967.
34. Shirayoshi Y, Nose A, Iwasaki K, Takeichi M (1986) N-linked oligosaccharides are not involved in the function of a cell–cell binding glycoprotein E-cadherin. *Cell Struct Funct* 11(3):245–252.
35. Cary LC, et al. (1989) Transposon mutagenesis of baculoviruses: Analysis of *Trichoplusia ni* transposon IFP2 insertions within the FP-locus of nuclear polyhedrosis viruses. *Virology* 172(1):156–169.
36. Ding S, et al. (2005) Efficient transposition of the piggyBac (PB) transposon in mammalian cells and mice. *Cell* 122(3):473–483.
37. Fraser MJ, Cary L, Boonvisudhi K, Wang HGH (1995) Assay for movement of Lepidopteran transposon IFP2 in insect cells using a baculovirus genome as a target DNA. *Virology* 211(2):397–407.